ARTICLES

Relaxation Dynamics in the Excited States of LDS-821 in Solution

Dipak K. Palit,* Ajay K. Singh, A. C. Bhasikuttan, and Jai P. Mittal†

Radiation Chemistry and Chemical Dynamics Division, Bhabha Atomic Research Centre, Mumbai 400 085, India

Received: November 9, 2000; In Final Form: February 26, 2001

Relaxation dynamics in the excited electronic state (S_1) of LDS-821 have been studied in aprotic and alcoholic solvents with pico- and subpicosecond time resolution using pump−supercontinuum probe transient absorption technique. Steady-state absorption and fluorescence as well as the time-resolved transient absorption/stimulated emission spectra and the temporal dynamics monitored at different wavelengths mainly reveal the features of a two-mode kinetic process in the S_1 state—conversion of the locally excited (LE) state to the twisted intramolecular charge-transfer (TICT) state. A short (<1 ps) rise time of stimulated emission monitored at the shorter wavelength band, is the signature of the barrierless skeletal stretching motion along the "valley-like" region of the potential energy surface (PES) of the S_1 state in the Franck−Condon (FC) region to attain a metastable untwisted configuration, called the LE state. The decay time of the LE state is equal to the rise time measured at the longer wavelength band, assigned to the TICT state. The linear dependence of the rate of the LE → TICT conversion process on the inverse of viscosity of the solvent indicates that this low-energy barrier crossing process is accompanied by a torsional motion about the free double bond of the molecule. The solvation time of the TICT state in different solvents has been seen to be nearly equal to the growth lifetime of the TICT state but much shorter than the longitudinal relaxation time of the solvent. These facts indicate that the rate of the LE → TICT process is mainly controlled by the contribution from the intramolecular modes rather than the solvation.

1. Introduction

Recently, large size electron donor−acceptor (EDA) molecules have shown promising applications in optical sensors and optical switches. Following optical excitation, such a molecule in condensed phase undergoes a numerous number of intra- and intermolecular processes taking place in the pico- and subpicosecond time domains.[1−5] However, among them three are the most important ones, in which the dynamics of the solute−solvent interaction play a significant role in determining the fate of the excited state of the solute and hence the rates of photophysical and photochemical processes undergone by it. These processes are energy exchange between the solute and the solvent molecules via vibrational relaxation or, more specifically, vibrational cooling, the solvation of the excited state via reorganization of the solvent molecules following the formation of the excited state, and conformational relaxation or isomerization. All these processes take place in ultrafast time scale and can be followed by probing the relaxation dynamics of the electronically excited molecules in solution.

The EDA molecules undergo a large change in dipole moment upon electronic excitation and this change in charge distribution in the excited state puts it out of equilibrium with its solvent environment. The subsequent solvent relaxation, called the solvation, is revealed by optical dephasing and dynamic Stokes' shift of the fluorescence maximum. Hence, optical spectroscopy provides a window onto microscopic solvation dynamics.[6−9] Ultrafast solvation dynamics in polar liquids has been an attractive and fascinating challenge for the theoreticians and the experimentalists as well, since the solvation process may control the dynamics of charge-transfer and other condensed phase chemical reactions. A popular method of studying the solvation dynamics is to measure the shift of the emission spectrum of the solute molecule as a function of time. If the charge-transfer process in the excited state of the molecule is ultrafast, then the solvation phenomena is the characteristic of the solvent and it is completed within a few tens of a picosecond. However, if the solute molecule is not quite rigid and two or more chromophore groups are connected via single or double bond(s), the molecule undergoes conformational changes, in case the barriers associated with the same processes in the excited state are less than a few kcal mol^{-1}. These processes also take place in the same time domain as the solvation.[10] In vibrational relaxation process, the vibrationally hot S_1 state is cooled by the collisional energy-transfer process to the solvent molecules, on a time scale ranging from a picosecond to a few tens of a picosecond depending on the nature of the solute, solvent and the amount of excess energy.[11−14] For example, in the case of IR-125,[15] HITC,[16] and *trans*-stilbene[17] molecules in the S_1 state, this process occurs in the 1−10 ps range.

Hence, it is obvious that in many of the molecular systems, as complex as the EDA molecules, the processes, like confor-

* To whom correspondence should be addressed. E-mail: dkpalit@apsara.barc.ernet.in. Fax: 091-22-550 5151.

† Also affiliated as honorary professor with the Jawaharlal Nehru Centre for Advanced Research, Bangalore, India.

10.1021/jp004142r CCC: $20.00
Published on Web 06/07/2001

mational relaxation, solvation dynamics, and vibrational relaxation, may occur simultaneously, and it should be challenging to study one of these processes and avoid the interference from the other two processes. Although a great deal of effort has been put in measuring solvation dynamics without complication of vibrational relaxation, in many cases confusion remains whether the relaxation process measured in a particular molecule is entirely due to the solvation process and the probe molecule used is an ideal one for studying solvation dynamics. However, studies of pure vibrational relaxation in excited electronic states by eliminating the effects of solvation dynamics have been few. Martin and Hartland recently investigated the vibrational relaxation dynamics in the excited electronic state of HITC by transient bleach/stimulated emission experiments.[16] Also, Elsasser and co-workers recently reported the study on vibrational relaxation dynamics on IR-125.[15]

Recently, studies on styryl dyes have received widespread interest because of their applications as optical sensitizers of silver halide colloids in photographic processes,[18] laser dyes,[19] fluorescent probes in biochemical procedures,[20] and biosensors.[21] However, these molecules are characterized by a short excited-state lifetime (5 ps to nanoseconds) and therefore by a low fluorescence quantum yield (<0.1).[22] This low yield is a consequence of an ultrafast nonradiative process that has been attributed to photoinduced trans−cis isomerization about one of the C═C bonds of polymethine chain.[23] Also, it is established that the emissive state of the ionic styryl dyes is characterized by a charge shift from the styryl group to the benzothiazolinium acceptor group. This charge shift is accompanied by a change in dipole moment of the ionic dye system and this consequently provides the driving force for solvation.[24−27]

Excited-state relaxation dynamics of the LDS series of styryl dyes have been the subject of many investigations by different groups. Fleming and co-workers used the excited relaxation dynamics of LDS-750 to probe the solvation dynamics.[24,25] Ernsting and co-workers have reported, on the basis of femtosecond transient absorption measurements, that the ultrafast excited-state dynamics of LDS-750 can be analyzed in terms of an isomerization reaction and so may not reflect solvation dynamics.[28] However, recently Yoshihara and co-workers reported their study on the dynamics of fluorescence Stokes' shift of LDS-750 in liquid aniline.[29] They concluded that although the spectral correlation function is reasonably well described by solvation dynamics, the time dependence of the shape of the time-resolved spectra could be explained if the solvent dynamics is the rate controlling process in both solvation of the increased dipole moment of the excited state of LDS-750 and the stabilization of a distribution of solute conformers in the excited state. Relaxation processes in LDS-821 dye and a few more dyes of this class have been studied by Zhong et al. by a time-resolved stimulated emission method.[30] Two kinds of relaxation processes in this type of dye molecule have been observed in different solvents: the intramolecular redistribution of energy with a short time constant less than 500 fs and another process taking place on the picosecond time scale, which have been assigned to the cooling of vibrationally hot molecules in the S_1 state.[30] However, they observed that the rates of these two processes strongly depend on the solvents and suggested that this may result from solvent-induced structural modification of the dye molecules.

In view of these conflicting ideas regarding ultrafast relaxation processes in the excited state of LDS dyes, it becomes important to reinvestigate the different kinds of relaxation processes these molecules undergo in the excited state using an ultrafast technique that will enable us to have information about spectral as well as temporal dynamics directly. We have chosen LDS-821 dye, also known as styryl 9M (molecular structure is presented in Scheme 1), for studying its excited-state dynamics by the transient absorption spectroscopic technique using white light continuum as the probe. The transient absorption spectra measured after dispersing the continuum probe in a polychromator provide spectral information regarding excited-state absorption, ground-state bleaching due to light absorption and stimulated emission as well as the temporal dynamics of these processes.[16,35] In the fluorescence band, the continuum light is amplified by stimulated emission and it has been shown earlier by many groups of scientists that this stimulated emission may provide the complete information about the dynamics of the fluorescing state since its intensity is proportional to the population of the fluorescing state as well as the spectral shape is related to the vibrational state distributions.[16,28,30,31] However, in many cases, for stimulated emission, if spectrally overlapped by excited-state and/or ground-state absorption bands, one should be careful to extract correct spectral and dynamical information about the excited state.

SCHEME 1

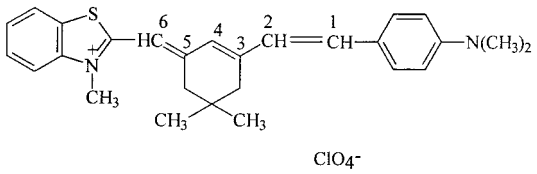

LDS 821 dye

2. Experimental Section

LDS-821 (2-(6-*p*-(dimethylamino)phenyl)-2,4-neopentylene-1,3,5-hexatrienyl)-3-methylbenzothiazolium perchlorate) (Scheme 1) was used as received from Exciton. Solvents were of UV-spectroscopy or guaranteed reagent grade from Spectrochem, (Mumbai, India) and were used without further purification.

Steady-state absorption spectra were recorded with a Shimadzu model UV-160A spectrometer. To record the fluorescence spectra at room temperature (298 K), 532 nm laser pulses of 35 ps duration and 0.5 mJ energy per pulse from an active-passive mode-locked Nd:YAG laser (continuum, model YG-501C-10) were used for excitation of the samples (optical density ∼0.3) taken in a quartz cuvette of 1 cm path length. The fluorescence was collected at a direction perpendicular to that of excitation through an optical fiber, dispersed through a spectrograph, and detected by a dual diode array based optical multichannel analyzer (Spectroscopic Instruments). The fluorescence spectra have not been corrected for the spectrometer response. However, the error incurred by not applying corrections was assessed by comparing the reported corrected spectra of IR-140 in ethylene glycol (EG)[32] and it has been seen that for the wavelength range of interest here, the resulting correction is negligible and has little effect on the data being reported here. The fluorescence quantum yields were determined by comparing to that of quinizarin in ethanol solution ($\phi_f = 0.11$).[33] For measuring the fluorescence spectra in solid matrices at liquid nitrogen temperature (77 K), the samples were taken in a quartz tube of 4 mm diameter and put into liquid nitrogen in a dewar and the spectra were recorded in the same manner as mentioned above.

Three different time-resolved techniques have been used to study the dynamics of the excited state. The fluorescence

lifetimes have been measured by a time-correlated single photon counting spectrometer having 20 ps time resolution and has been described elsewhere.[34] The transient absorption spectra with 35 ps time resolution have been recorded by a picosecond laser flash photolysis apparatus the details of which are available in ref 35. The information on the dynamics of interest occurring on a time scale faster than 50 ps have been obtained using a home-built subpicosecond transient absorption spectrometer, which can be described here in brief as follows: the 100 pJ pulses of 70 fs duration at 620 nm generated in an argon ion pumped colliding pulse mode-locked (CPM) dye laser have been amplified to about 100 μJ pulses of 100 fs duration in a five stage dye amplifier pumped by a Nd:YAG laser (280 mJ at 532 nm, 30 Hz). About 10% of the energy output from the amplifier ($\sim$10 μJ) was used to excite the sample (optical density $\sim$0.5) taken in a flow through cell of 2 mm path length. The residual fundamental has been used to generate the white light continuum (400−950 nm) in a flowing water medium of 1 cm path length and the polarization direction of the probe was fixed at the magic angle, i.e., 54.7°, with respect to that of pump polarization. The angle between the pump and probe pulses falling on the sample is about 20° and the spot sizes of the two beams at the sample were about 1 mm. The transient absorption spectra were recorded using the optical multichannel analyzer and the decay dynamics at a particular wavelength region (10 nm width) were monitored using two photodiodes coupled with the boxcar integrators. The overall time resolution of the absorption spectrometer was measured to be about 300 fs by measuring the growth of the negative absorption signal at 650 nm due to bleaching in the ground state for malachite green in ethylene glycol and the same was used to determine the zero delay position between the pump and the probe pulses. The spectra were not corrected for the deformation due to the effect of the group velocity dispersion of the probe pulse due to the optical materials used in the spectrometer. However, we made the measurements of the delays, at which the different colors of the probe pulse reach the sample, at a few wavelengths and they confirmed that the transient spectra recorded later than 0.5 ps after the pump pulse in 650−900 nm region, while the zero delay position has been set at 650 nm, should reveal the information regarding the evolution of the transient species. However, the temporal dynamics monitored at a particular wavelength with ca. 10 nm width, reveal the quantitative evolution of a particular transient species with a time resolution of about 300 fs. The temporal dynamics have been analyzed by fitting the temporal profile by iterative deconvolution with the instrument response function of Sech^2 type having fwhm of 300 fs.

3. Results

3.1. Steady-State Absorption and Fluorescence Studies. Figure 1 displays a few typical sets of steady-state absorption and fluorescence spectra of LDS-821 in a few of the solvents studied here at room temperature and also the emission spectra in solid matrices at 77 K. The absorption spectra are structureless and broad, having half-widths of about 4000 cm^{-1}. The large bandwidth and the large extinction coefficient values ($\sim$5.0 $\times$ 10^4 mol dm^{-3} cm^{-1} at 585 nm in ethanol)[36] for the absorption probably indicate involvement of charge transfer, most likely involving partial donation of the amino lone pair to the charged methylbenzothiazolium moiety through the conjugated π-bonded alkene chain.[24] The steady-state absorption spectra of LDS-821 in different solvents show systematic variations as a function of polarity (Table 1). The broadness of the absorption spectrum

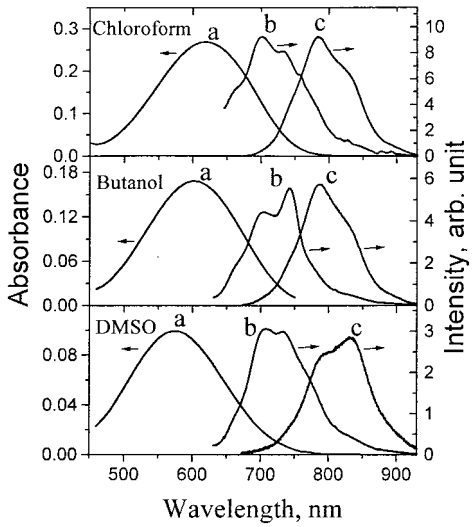

Figure 1. Steady-state absorption spectra (a), emission spectra in solid matrices at 77 K (b), and fluoresecnce spectra at room temperature (c) in chloroform, *n*-butanol and DMSO.

may arise due to contribution from more than one electronic state to the absorption spectrum. The other reason is that it probably reflects a broad distribution of conformers (solvent−solute or intramolecular) in the ground state.

The emission spectra in each solvent recorded at room and liquid nitrogen temperatures are significantly different, the former ones being very much red shifted with respect to the latter ones. In both the cases, the emission spectra show shoulders at both sides of the peak and the relative heights of the shoulders and the peak are solvent dependent. However, the emission spectra recorded at both the temperatures are considerably narrower (fwhm $\sim$ 1300 cm^{-1}) than the absorption spectra. With increasing solvent polarity, as measured by the reaction field factor, $\Delta F(\epsilon_0,n)$,[9,37] the maxima of the absorption spectra shift to the blue. Such behavior is indicative of decreased stabilization of the Franck−Condon (FC) S_1 state relative to the ground (S_0) state by the more polar solvent and hence lower μ value of the former state as compared to the latter is evident.

The solvent dependent shape of the emission spectra also indicates the possibility of the presence of more than one conformer, either or both in the ground and excited electronic states. The maximum of the emission spectrum recorded in each of the solvents at room temperature shows a large red shift, more than ca. 180 nm with respect to the absorption maximum in the corresponding solvent. This large Stokes' shift between the maxima of the absorption and emission spectra recorded at room temperature indicates that certainly the FC state is not the emitting state. The steady-state fluorescence maximum shifts to red due to an increase in solvent polarity, which is evident from Table 1. However, no reasonable correlation has been found between the fluorescence peak maxima and the solvent polarity parameter, $\Delta F(\epsilon_0,n)$. The same is true for the dependence of the Stokes' shift parameter ($\Delta\nu = \nu_{abs} - \nu_{em.}$, cm^{-1}) on $\Delta F(\epsilon_0,n)$. The possible reason behind the lack of correlation between the fluorescence maxima (ν_{em}) or $\Delta\nu$ and the solvent polarity parameter, $\Delta F(\epsilon_0,n)$ (or any other parameter, e.g., π^* or E_T^N)[38] (Table 1), is the emission from more than one conformer formed following optical excitation. Since the solvent effect on the fluorescence maxima of the undecomposed spectra is not a simple reflection of the solvent dependence of a particular excited-state conformation, the spectral shape as well as the solvent shift also depend on the relative quantum yields of the conformers. The total fluorescence quantum yields (ϕ_f)

TABLE 1: Photophysical Properties of LDS-821

solvents & polarity parameters[a] (ΔF, π^*, E_T^N)[a]	absorption λ_{max}, nm[b]	fluorescence λ_{max}, nm[c]	stim. emission λ_{max}, nm[d]	$\Delta\nu_1$,[e] cm^{-1}	ϕ_f	τ_f,[f] ps	$10^{-8}k_R$,[g] s^{-1}	$10^{-9}k_{NR}$ [h] s^{-1}
CF (0.29, 0.69, 0.259)	619	785	804	3416	0.10	1030	0.98	0.87
DCM (0.47, 0.73, 0.309)	632	797	810	3276	0.105	1340	0.78	0.67
acetone (0.65, 0.62, 0.355)	570	797	806	5136	0.044	450	0.98	2.12
ACN (0.71, 0.66, 0.46)	563	792	819	4796	0.035	570	0.61	1.69
DMF (0.67, 0.88, 0.386)	571	830	835	5465	0.037	580	0.64	1.66
DMSO (0.66, 1.0, 0.444)	574	834	842	5432	0.045	558	0.81	1.71
methanol (0.71, 0.60, 0.762)	574	792	820	4987	0.038	350	0.99	2.53
ethanol (0.67, 0.54, 0.654)	588	811	817	4997	0.04	400	1.00	2.40
1-propanol (0.63, 0.52, 0.617	596	798	814	4493	0.041	500	0.82	1.92
2-propanol (0.63, 0.48, 0.546)	593	797	813	4677	0.036	490	0.74	1.97
n-butanol (0.63, 0.47, 0.586)	601	788	812	4316	0.03	585	.51	1.66
1-pentanol (0.57, −, 0.586)	606	787	812	3795	0.051	675	0.76	1.41
1-decanol (0.41, −,0.525)	600	780	810	3860	0.031	714	0.43	1.36
ethylene glycol (0.67, 0.92, 0.79)	580	792	825	4627	0.021	296	1.3	3.2

[a] Values are from refs 37 and 38. [b] Ground-state absorption. [c] Room-temperature fluorescence. [d] Maximum of the stimulated emission band observed at 35 ps after photoexcitation. [e] $\Delta\nu_1 = \nu_{max}(abs) - \nu_{max}$ (stim em). [f] lifetime of fluorescence monitored at 830 nm. [g] $k_R = \phi_f/\tau_f$; [h] $k_{NR} = (1 - \phi_f)/\tau_f$.

have been given in Table 1. Excluding the chloroalkane solvents, the ϕ_f values show very little variation with respect to polarity.

3.2. Time-Resolved Studies. *3.2.a. Fluorescence Lifetime Measurements.* The fluorescence lifetimes (τ_f) have been determined by single photon counting by monitoring the fluorescence decay at two wavelengths, 770 and 830 nm on the fluorescence spectra of LDS-821. The fluorescence decay function is seen to be monoexponential in all the solvents when monitored at 830 nm but double exponential at 770 nm. Among the two components associated with the fluorescence decay at 770 nm, the one with the larger lifetime is seen to be similar to the one obtained from the measurement at 830 nm in the corresponding solvent. But the shorter component being very short (<20 ps), shorter than or comparable to the time resolution of the equipment, is not reproducible from different measurements and hence not given in Table 1; only the lifetime of the longer component is given, which may be considered as the lifetime of the S_1 state of the most stable conformer of LDS-821 molecule.

Lifetimes (τ_f) are longer (about 1 ns) in chloroalkane solvents but in polar solvents the lifetimes are short and vary in the range 300−600 ps (Table 1). Radiative (k_R) and nonradiative (k_{NR}) rate constants have been calculated by assuming that the yield of the intersystem crossing to the triplet is negligible (see later), and the values are given in Table 1. In the alcoholic solvents, k_{NR} has reasonably good linear correlation with the inverse of viscosity of the solvent, η^{-1}, and it increases with a decrease in solvent viscosity. However, in nonalcoholic solvents, k_{nr} is not so well correlated with η^{-1}. These facts indicate that in the deactivation process of the S_1 state, in addition to the nonradiative relaxation process involving intramolecular rearrangements, e.g., isomerization, which is expected to be hindered by the solvent viscosity, solvation phenomena as well as other specific kinds of solute−solvent interactions might also play significant roles. In addition, the lack of good correlation between k_{NR} and η^{-1} is probably due to the fact that the quantum yield of the total emission determined experimentally is not due to emission from a single isomer, for which the lifetime of a few hundred picoseconds has been determined. The fluorescence yield reported in the Table 1 is the total emission yield from more than one isomers formed following optical excitation (see later).

3.2.b. Transient Absorption Studies. Figure 2 shows the time-resolved transient absorption spectra recorded in the subpicosecond time domain following photoexcitation of LDS-821 in chloroform solution by 620 nm laser pulses of subpicosecond duration. The transient spectrum recorded at 0.5 ps (curve 1 in Figure 2) shows several features: a positive absorption band at ca. 550 nm, which grows with an increase in time delay, a negative absorption band at 620 nm, probably due to ground-state bleaching but masked by the growing positive absorption band at 550 nm at later time, and a weak emission band having a peak at ca. 750 nm. This emission grows up initially (upto 2 ps) and then decays with a concomitant development of a new emission band having a peak at 800 nm. The latter continues to grow up to about 15 ps with no shift of the wavelength maxima of the stimulated emission band with time. The temporal evolution of the transient absorbance has been followed at 730 and 800 nm and is shown in the inset of Figure 2. The growth and decay lifetimes of the stimulated emission measured at 730 nm are 1 ± 0.2 and 4.5 ± 0.4 ps, respectively. The growth lifetime of the stimulated emission intensity monitored at 800 nm is 4.2 ± 0.2 ps. Because of the absorption bands, which are growing with increases in time delay at ca. 550 and 700 nm, overlapping with the band due to bleaching at ca. 620 nm, no attempt has been made to study the dynamics at these wavelengths. The good agreement between the decay lifetime

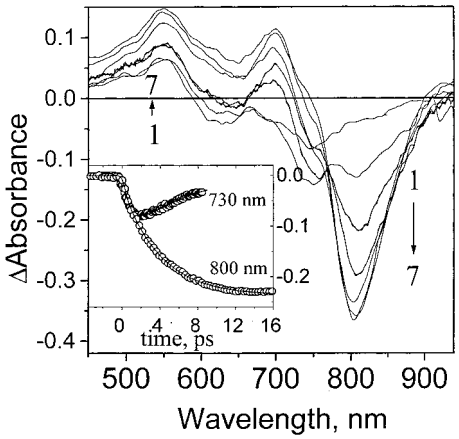

Figure 2. Time-resolved transient (absorption/stimulated emission) spectra of LDS-821 in chloroform due to excitation at 620 nm. The spectra are recorded at 0.5 (1), 1 (2), 2 (3), 5 (4), 10 (5), 15 (6), and 30 (7) ps time delays after the pump pulse. The inset shows the temporal evolution of the transient absorption/stimulated emission at 730 and 800 nm. At 730 nm the stimulated emission grows with a lifetime of 1 ps followed by a decay with lifetime of 4.5 ps. At 800 nm the stimulated emission grows with a lifetime of 4.2 ps.

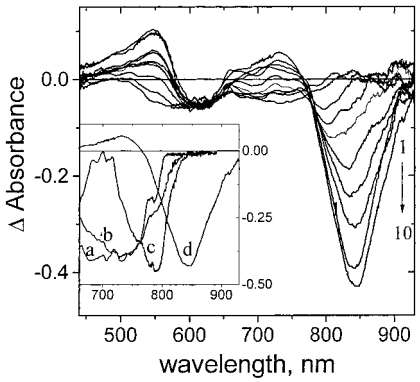

Figure 3. Time-resolved transient spectra of LDS-821 in DMSO due to excitation at 620 nm. The spectra are recorded at 0.5 (1), 0.7 (2), 1 (3), 1.5 (4), 2 (5), 3 (6), 5 (7), 8 (8), 10 (9), and 12 (10) ps time delays after the pump pulse. The inset shows the evolution of the stimulated emission spectra in 650−930 nm region, recorded at 0.5 (a), 0.7 (b), 1 (c), and 12 (d) ps time delays, as they have been normalized to approximately the same intensity at the wavelength maxima.

of the stimulated emission measured at 730 nm and the growth lifetime measured at 800 nm indicates that the state or the species having the stimulated emission band centered at 800 nm is formed due to decay of the state or the species having an emission band centered at 750 nm.

Figure 3 shows the time-resolved transient absorption spectra obtained due to photolysis of LDS-821 in DMSO in a subpicosecond time domain. In addition to the negative absorption band appearing in the 500−650 nm region due to ground-state bleaching, the transient spectrum (curve 1) recorded at 0.5 ps after the pump laser pulse shows a weak emission band in the 650−800 nm region with a maximum at ca. 700 nm. With an increase in time delay, this emission band disappears with a concomitant development of a positive absorption band in the same region as well as another emission band in the red side of the former (i.e., in the region 800−900 nm). With an increase in time delay, the wavelength maximum of this new emission band shifts gradually from ca. 800 nm, as it starts developing during ca. 1 ps delay, to 842 nm at 15 ps, when it is fully grown. The temporal dynamics of the transients monitored at 590, 730, and 850 nm have been shown in Figure 4. The negative absorbance at 590 nm due to ground-state bleaching increases following the instrument response limited rise time and does not show any recovery within the time of our measurements, i.e., up to about 20 ps. This indicates that the molecules excited do not come down to the ground state within this time interval. The temporal profile of the differential transient absorption monitored at 730 nm also shows the instrument response time limited rise of the stimulated emission, which subsequently disappears and is followed by the growth of a positive absorption with a lifetime of about 4.0 ± 0.4 ps. However, the temporal profile recorded at 850 nm shows a clean growth with a lifetime of 3.9 ± 0.2 ps. The inset of Figure 3 also shows a comparison of the spectra of the transients monitored at four different times as normalized to the same peak heights. The inset shows only the changes in the shapes of the stimulated emission spectra of the transients at different time delays. At 0.5 ps the transient emission spectrum is very broad, the peak intensity extending from 670 to 750 nm. Because of overlapping of this emission band with that due to bleaching, its actual shape could not be ascertained. At later times the width of the spectrum becomes narrower and the peak wavelength shifts to ca. 790 nm within 1 ps and later to 840 nm after about 15 ps. Within this time period, the growth of the emission intensity at 840 nm is also complete. However, since the bleaching band arising due to

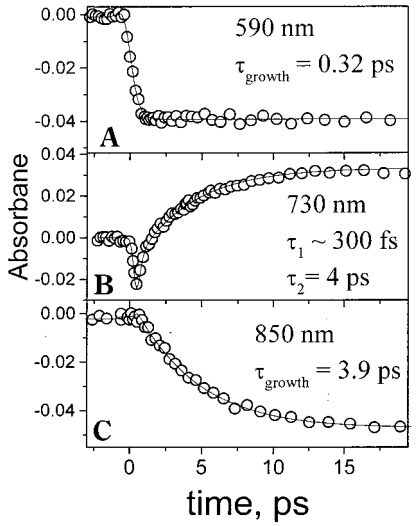

Figure 4. Temporal evolution of the transient absorption/stimulated emission due to photoexcitation of LDS-821 in DMSO monitored at 590 (A), 730 (B), and 850 (C) nm. At 590 nm, the bleaching due to ground-state depletion shows a rise with instrument response time limit (τ_{growth} = 0.32 ps) and does not show any recovery up to 20 ps. At 730 nm the temporal evolution of the stimulated emission shows a fast rise with instrument response time and subsequently a growth of transient absorption with lifetime of 4 ps. At 850 nm the stimulated emission grows with a lifetime of 3.9 ps.

TABLE 2: Solvent Properties and Time Constants of LDS-821

solvents	τ_L, ps[a]	$\langle\tau\rangle_{probe}$, ps (probe)[b−d]	τ_g, ps	τ_1 (ps), τ_2 (ps)	$\langle\tau\rangle_{solv}$, ps
CF		2.8	4.0	−	
DCM		0.5	1.8	−	2.1
ACN	0.2	0.26 (coumarin) 0.4 (LDS 750)	1.5	−	1.5
DMSO	2.1	1.79 (coumarin) 3.1 (LDS 750)	4.0	−	2.5
MeOH	9.2	5.0 (coumarin) 2.7 (DCM) 3.3 (LDS 750)	2.0	0.4, 3.5	1.8
ethanol	60	16 (coumarin)	6.5	1.0, 6.5	3.6
propanol	75	26 (coumarin)	16	1.1, 12.3	10.6
butanol	120	63 (coumarin) 66 (LDS-750)	14	1.2, 12.3	11.1
pentanol		103 (coumarin)	22.0	−	20
ethylene glycol	86	15.0 (coumarin) 8.0 (DCM)	17	1.5, 52	17.1

[a] Reference 7. [b] Reference 51. [c] Reference 24. [d] Reference 43.

ground-state depletion at 600 nm has not shown any recovery within the time up to 15 ps, the relaxation process we observe here must be taking place in the fluorescing state or any other excited state preceding the fluorescing state.

The excited-state dynamics of LDS-821 have been monitored in a few other solvents, as mentioned in Table 2. The gross features of the time-resolved transient absorption characteristics are more or less similar in other solvents as those described in the case of DMSO. In each of the solvents, the temporal dynamics of the transient species monitored at 730 nm shows a very fast rise ($\tau_{growth} \leq 1$ ps) of the stimulated emission intensity and then decay, the lifetime of which nearly matches with that determined by monitoring the growth in the 800−850 nm region. In chloroform and ethylene glycol, the growth of the stimulated emission at 730 nm is relatively longer (ca. 1 ps) as compared to that in other solvents, e.g., in acetonitrile, methanol, and DMSO, in which this process is instrument response time limited (i.e., ≤300 fs). The growth lifetime (τ_g)

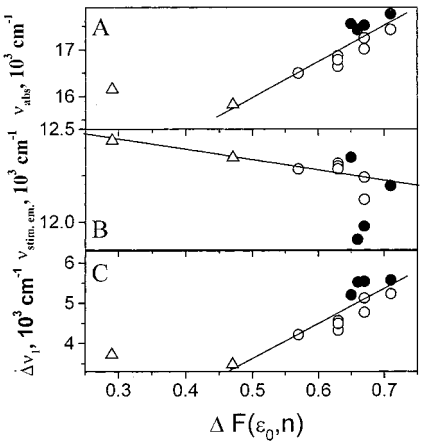

Figure 5. Frequency maxima for steady-state absorption, ν_{abs} (A), stimulated emission, $\nu_{stim\ em}$ (B), and Stokes shifts, $\Delta\nu_1$ (between the steady-state absorption and stimulated emission) (C), are plotted as a function of the reaction field factor, $\Delta F(\epsilon_0,n)$. Alcoholic solvents are shown as open circles (○), the aprotic or simple dipolar solvents as filled circles (●), and the chloro solvents as open triangles (△). The lines represent the least-squares fits of the data with the solvents excluding chloroform in (A) and (C) and DMF and DMSO in (B).

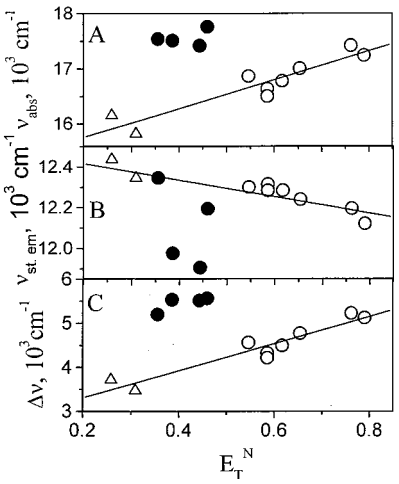

Figure 6. Frequency maxima for steady-state absorption, ν_{abs}, (A), stimulated emission, $\nu_{stim\ em}$, (B) and Stokes' Shifts, $\Delta\nu_1$, (C) are plotted as a function of the solvent polarity parameter, E_T^N. Alcoholic solvents are shown as open circles (○), the aprotic or simple dipolar solvents as filled circles (●) and the chloro solvents as open triangles (△). The lines represent the least-squares fits of the data with the solvents excluding the four aprotic dipolar solvents, namely, acetone, acetonitrile, DMF and DMSO.

of the stimulated emission, obtained by single-exponential fitting to the growth of the emission intensity monitored at 800−850 nm in different solvents, are given in Table 2.

The stimulated emission at 830 nm has been seen to decay in the picosecond time domain following photoexcitation by 532 nm laser pulses of 35 ps duration, and this decay lifetime has been observed to be nearly the same (within experimental error of about 5%) as that of the decay of the transient absorption monitored at 540 nm as well as the rate of bleaching recovery monitored at 600 nm. The lifetimes of the transient species obtained from these measurements have also been seen to agree well within experimental error with those determined by the single photon counting technique (Table 1). The isosbestic points in the time-resolved spectra between the positive and negative absorption bands indicate that at any time after about 35 ps of photoexcitation, only two states, namely the ground and the fluorescing states, are responsible for the entire spectrum and the ground state recovers nearly quantitatively after relaxation from the fluorescing state. Hence, this fact excludes the possibility of formation of any other intermediates between these two states, e.g., the triplet state or any other isomers in the excited state. The shapes of the stimulated emission spectra recorded after 35 ps are perfectly Gaussian without the presence of any shoulders seen in the steady-state emission spectra. This fact indicates that this emission band is due to the S_1 state of a single conformer species and the region of this stimulated emission band is not overlapped with that of the excited-state absorption of the same conformer species. The maxima of the stimulated emission bands and the Stokes' shift parameters, $\Delta\nu_1 = \nu_{abs} - \nu_{stim\ em}$, in different solvents have been given in Table 1. They show significant solvent dependence; e.g., the maxima are at 800 and 842 nm in chloroform and DMSO, respectively.

In Figure 5, maxima of steady-state absorption (ν_{abs}) and stimulated emission ($\nu_{stim\ em}$) and the Stokes' shift parameter, $\Delta\nu_1$, (Table 1) have been plotted as a function of the reaction field factor, $\Delta F(\epsilon_0,n)$, of the solvents. It is evident that although ν_{abs} and $\Delta\nu_1$ are reasonably well correlated (correlation coefficient, $R \geq 0.9$ in 13 solvents, i.e., $N = 13$, in both the cases) with $\Delta F(\epsilon_0,n)$ values of the solvents in both the alcoholic as well as nonalcoholic or simple dipolar solvents, excluding chloroform from the fit, the correlation between $\nu_{stim\ em}$ and $\Delta F(\epsilon_0,n)$ is very poor ($R = 0.82$ with $N = 12$). The decrease in stimulated emission frequency and increase in the value of $\Delta\nu_1$ with an increase in solvent polarity indicate that the fluorescing state is a CT state and the difference in dipole moments between that of the excited and ground states ($\Delta\mu$) has been calculated to be 9.8 D by using the Lippert−Mataga equation.[39]

Thus, although both simple dipolar and alcoholic solvents could be adequately modeled in terms of continuum dielectric descriptions of solvation, there is considerable scatter in the data. This fact probably indicates that in addition to the more obvious source of Stokes' shift, modulation of the interaction between the permanent charge distributions of the solute and solvent, any other special kind of solvent interaction, e.g., interaction via hydrogen bonding or donation of electron pair, may also contribute in the stabilization of the fluorescing state. Hence to gain information about this kind of solute−solvent interaction, these three photophysical parameters (namely ν_{abs}, $\nu_{stim\ em}$ and $\Delta\nu_1$) have been correlated with the two most popular empirical scales of solvent polarity, π^* and E_T^N.[9,38] We could not find any reasonable correlation between any of these three parameters and the π^* polarity parameter of the solvents. Figure 6 shows the correlation between these three parameters and the E_T^N values of the solvents used here. The solvents (Table 1) can be roughly divided into three main categories according to their E_T^N values depending on the specific solute−solvent interactions: (i) protic hydrogen-bond donating (HBD) solvents with E_T^N values in the range (0.5 to 1), i.e., the alcohols; (ii) diploar aprotic non-HBD solvents with E_T^N values 0.3−0.5, i.e., acetone, acetonitrile, DMF, and DMSO; (iii) apolar aprotic non-HBD solvents with E_T^N values in the range (0 to 0.3), i.e., chloroform and DCM.[38] The plots in Figure 6 show that all the three photophysical parameters are differently correlated in dipolar aprotic solvents than in other solvents. In these solvents the values of the Stokes' shift parameter is unusually larger than those in other solvents. The dipolar aprotic solvents used here are usually good electron pair donating solvents and hence much larger shifts in these solvents can be attributed to the higher solvation energies due to solvation of the cation. This fact indicates the relative importance of electronic contribu-

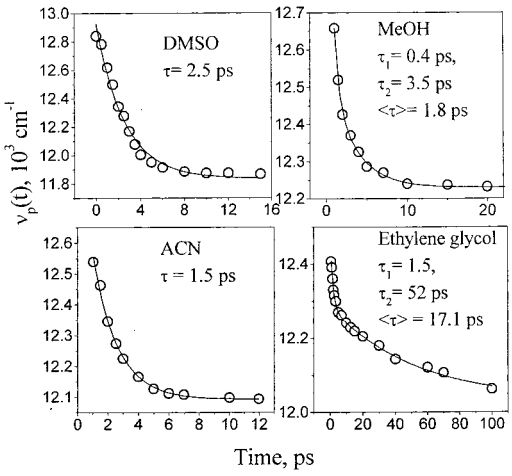

Figure 7. Stimulated emission peak maxima, $\nu_p(t)$, plotted as a function of time delay, t, between the pump and the probe pulses in four solvents. The single or double-exponential fit function with the lifetimes given illustrates the solvation dynamics of the TICT state formed in the S_1 state of LDS-821. In methanol and ethylene glycol, the solvation dynamics show bimodal behavior. The average solvation time, $\langle\tau\rangle_{solv}$, has been calculated by using eq 2.

tions to the stabilization of the S_1 state, from which the stimulated emission originates, rather than the hydrogen bonding interaction.

Now the question is whether the growth of the emission band, which is accompanied by a dynamic Stokes' shift, is due to formation of an intramolecular charge-transfer state and its solvation, or due to vibrational relaxation in a newly created excited state, as predicted by Zhong et al.[30] Since we observe this shift only in polar solvents, but not in relatively less polar chloroform, the growth of the emission band and the dynamics Stokes' shift in the 800−850 nm regime could possibly be assigned to the formation of an intramolecular charge-transfer (ICT) state and its simultaneous solvation. The dynamic Stokes' shift in polar media is represented by the normalized spectral response function $C(t)$, as defined by[40−42]

$$C(t) = \frac{\nu(t) - \nu(\infty)}{\nu(0) - \nu(\infty)} \tag{1}$$

where $\nu(0)$, $\nu(t)$, and $\nu(\infty)$ are the peak frequencies of the stimulated emission band due to the TICT state at zero time (i.e., in this case it is the time when the barrier crossing process just started), at time t after this zero time, and at very long time when no more shift is observed, respectively. The dynamic Stokes' shift also can be represented by either the time dependence of the peak frequency, $\nu_p(t)$, or the first moment $\nu(t)$ of the log-normal fit to the stimulated emission spectrum.[9] It has also been discussed that in the case of C-153, there is very little difference in the time behavior due to solvation of the two parameters, $\nu_p(t)$ and $\nu(t)$,[9,43] and the time dependence of $\nu_p(t)$ is the same as that for $C(t)$.[43]

In Figure 7, we depict $\nu_p(t)$ as a function of time for a few of the solvents. The reason that we have shown the time dependence of $\nu_p(t)$ rather than $C(t)$ is that we want to avoid the error that may arise in $C(t)$ due to uncertainty in the frequency of the charge-transfer emission at $t = 0$. Also we verified in a few of the cases that the time dependence of $\nu_p(t)$ is equal to that for $C(t)$ within experimental error (10%). In nonalcoholic solvents the time behavior of $\nu_p(t)$ could be fitted to a single exponential decay function reasonably well, but in alcoholic solvents the same could be fitted well only with a double-exponential function. The lifetimes of the two components, τ_1 and τ_2, obtained in different solvents are given in Table 2. Such bimodal behavior of $C(t)$ or $\nu_p(t)$ in alcoholic solvents has been observed by many of the groups studying solvation dynamics using various kinds of probes.[7,24,25] However, here we are not concerned about the significance of the multicomponent behavior of the solvation phenomena but only the average solvation times, $\langle\tau\rangle_{solv}$, determined either by single-exponential fitting of the $\nu_p(t)$ curves or by calculating the same from the decay times obtained by double-exponential fit using eq 2,[44]

$$\langle\tau\rangle_{solv} = \frac{a_1\tau_1 + a_2\tau_2}{a_1 + a_2} \tag{2}$$

where τ and a represent the lifetime and the corresponding amplitude due to a particular solvation component. The $\langle\tau\rangle_{solv}$ values determined are given in Table 2 along with the longitudinal relaxation time, τ_L, of the solvents and the solvation times, $\langle\tau\rangle_{probe}$, as determined earlier by other groups using other kinds of probes.[7−9,24,43,45]

4. Discussion

Scheme 1 shows that in the LDS-821 molecule, a hexamethine hemicyanine dye, the (dimethylamino)phenyl (donor) group is connected to the methylbenzothiazolium (acceptor) group by a π-conguated spacer group consisting of a polymethine chain having three ethylenic units. However, among these three ethylenic units, two are parts of a rigid cyclohexenyl ring and the other is flexible and only the latter is able to undergo torsional motion to take part in the trans−cis isomerization process. It is known that the length of the polymethine chain controls the photophysical properties of this kind of donor−acceptor type of molecule.[16,30,46] The influence of a longer polymethine chain (here it is a chain of six π-conjugated carbon atoms) enhance the stability of the π-system by electronic delocalization. The results of the reaction path computations for such a long conjugated polymethine cyanine system (e.g., penta- and heptacyanines) suggests that the ultrafast evolution of the excited state of these chromophores can be described using the two-state two-mode model, which has been proposed to explain the primary events corresponding to the light-induced trans−cis isomerization of a retinal protonated Schiff base (PSB) chromophore embedded in proteins.[47,48] In this model, only the ground state (S_0) and the first excited singlet $\pi-\pi^*$ state (S_1) are involved in the reaction. Upon excitation to the S_1 state, the molecule follows a path in which different vibrational modes are populated sequentially. The first mode is totally symmetric and drives the initially planar system out of the FC region through a skeletal stretching. The second vibrational mode is totally nonsymmetric and is dominated by torsional motion about one of the central double bonds of the system. This two-mode motion, in turn, leads the system toward a *ca.* 90°-twisted configuration, where the S_0 and S_1 potential energy surfaces cross at a conical intersection, thus triggering an extremely efficient $S_1 \rightarrow S_0$ decay. A detailed analysis of the computed path of the cyanines indicates that the structure of the S_1 potential energy surface in the vicinity of the FC point is "valley-like" and the initial relaxation occurring in the FC region is fully dominated by the barrierless symmetric skeletal deformation mode.[47] The extended valley-like shape of the S_1 surface along the stretching coordinate prevents a fast stretching-torsional coupling. In the case of the long chain polymethine cyanines (with the number of CH units $n \geq 5$), the stretching modes and the torsoinal modes are completely uncoupled and

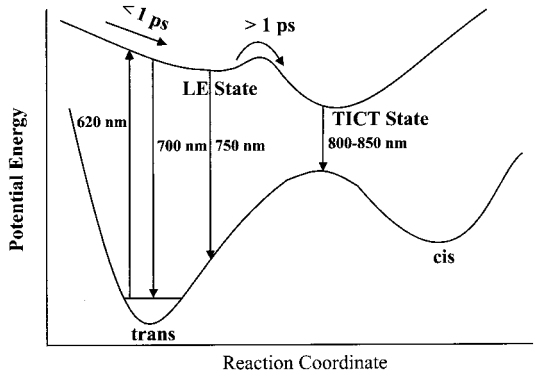

Figure 8. Potential energy surface for the two-state two-mode model for the relaxation of LDS-821 molecule in the S_1 state.

hence the initial relaxation will be fully dominated by the stretching mode, and the torsional mode will be populated only after partial equilibration at a metastable untwisted intermediate. This intermediate then undergoes trans−cis isomerization via the torsional motion about the C═C bond and the dihedral angle changes from 0° to about 100°. This process corresponds to an activated barrier crossing process.

The PES for the two-state two-mode model for the relaxation process in the S_1 state of LDS-821 molecule has been shown in Figure 8.The time-resolved spectra as well as the temporal dynamics of the stimulated emission monitored at different wavelengths, as shown in the Figures 2−4 mainly reveal the features of two-mode kinetic process—conversion of the LE state to the TICT state. For short wavelength detection, e.g., at 730 nm, we observe the S_1-state relaxation in the region close to the FC point. A short or nonexistent (i.e., ≤1 ps) rise time and very fast spectral evolution in this higher energy spectral regime (700−800 nm) are the signatures of the transient species evolving along the skeletal deformation coordinate in the valley-like region to attain the metastable untwisted intermediate conformation, called the LE state. This assignment is supported by the difference in the steady-state emission spectra recorded in solid matrices at 77 K and in solutions at room temperature (Figure 1). For example, in the DMSO glass matrix at 77 K, in which the molecule is not able to undergo any kind of conformational relaxation, the steady-state emission spectrum has a peak at ca. 705 nm. But, in time-resolved experiments, we observed a broad emission band with a peak at ca. 700 nm, which could probably be assigned to the emission originating from the FC excited state, having the same conformation as in the ground state. However, after about 1 ps the spectral shape of the stimulated emission band changes to one having a width narrower than that of the spectrum recorded at 0.5 ps and an emission peak at ca. 800 nm. This process is followed by torsional motion about the free double bond (C_1═C_2) accompanied by the intramolecular charge transfer. The longer rise time measured at a longer wavelength regime (800−850 nm) is the signature of the motion that corresponds to torsion, leading to the TICT minimum. Hence, the growth of the stimulated emission observed in the 800−850 nm wavelength regime in different solvents could be assigned primarily to the population kinetics due to LE → TICT interconversion process, and the parameter τ_g (Table 2), to the rate of this process. The continuous shift of the peak of the stimulated emission band with an increase in time delay observed at this wavelength regime in polar solvents indicates the solvation of the TICT state produced. This S_1(TICT) state decays to the ground state at a much longer time scale (>300 ps).

The fast relaxation process, which is observed in the 700−800 nm wavelength region in the present system, cannot be assigned to the intramolecular vibrational (energy) relaxation (IVR) process, since the dyes of this class have been shown to undergo the IVR process in a time scale faster than 100 fs.[11,16,25,28,49] This process has also been reported in the case of other cyanine or hemicyanine dyes. For eaxmple, recently, Ernsting and co-workers reported that the intramolecular relaxation process in the S_1 electronic state of LDS-750 proceeds in two steps, $S_1 \rightarrow S_1' \rightarrow S_1''$.[28] To explain the higher energy gain band at early time (<200 fs), an intermediate isomeric state, S_1', which is formed within about 100 fs after excitation, has been predicted. Solvation of the excited state is followed by the crossover process, $S_1' \rightarrow S_1''$, the latter being the isomerized charge-transfer (CT) state. Bingeman and Ernsting, in their report on the study of solvation dynamics of DASPI, a short chain hemicyanine, observed an ultrafast component in the higher wavelength regime of the time-resolved stimulated emission spectra at early time (<200 fs) before the actual solvation process started.[31] In the case of both DASPI and LDS-750, being short chain (di- and trimethine) hemicyanines, the PES in the S_1 state near the FC region possibly is "ridge-like", rather than "valley-like" as in the case of long chain cyanines and also the LE → TICT process is barrierless.[47] Hence, both the formation and disappearance of the LE state are expected to be very fast in these chromophores. Martini and Hartland[16] reported the S_1-state relaxation process of HITC, a heptacyanine dye. The decay with <100 fs lifetime observed at higher energy regime has been assigned to IVR. At a longer wavelength regime, in addition to the slower process (≥1.7 ps) due to solvent-induced vibrational cooling, a component with 300 fs rise has been observed and the latter too has been assigned to a slower IVR, which has been predicted to be due to smaller coupling matrix elements or because of the coupled levels further away in energy. However, the latter process is certainly due to intramolecular relaxation, since the rise time is independent of the solvent. Probably this 300 fs growth could be assigned to the relaxation process occurring along the valley-like PES near the FC region forming the LE state, which subsequently cross over a barrier to form the twisted isomer in the S_1 state. In the present case, LDS-821 being an hexamethine hemicyanine and, in addition, two central C═C double bonds being part of a rigid structure, the formation of LE state via the early relaxation process is comparatively slower than those reported for other cyanines. The subsequent LE → TICT process too is expected to be slower because of a higher energy barrier due to the proximity of the only flexible C_1═C_2 bond to the (dimethylamino)phenyl (donor) group.[47]

We have looked for possible correlation between τ_g and $\langle\tau\rangle_{solv}$ and various measures of energetics and dynamics of solvation, some of which are listed in Table 2. It is important to note that in different solvents, the values of τ_g, the LE → TICT conversion times, are uniformly greater than or very nearly equal to the average solvation times, $\langle\tau\rangle_{solv}$ and these two parameters have good linear correlation in all kinds of solvents used here (Figure 9A, $R = 0.92$, $N = 10$). In addition, Figure 9B shows that the rate constants for the LE → TICT process, i.e., τ_g^{-1}, are well correlated with the inverse of the viscosities (η^{-1}) of the solvents ($R = 0.93$ with $N = 10$). The solid line in Figure 9B represents the linear fit function: $\tau_g^{-1} = 0.009 + 0.21\eta^{-1}$ or $\tau_g^{-1} \sim 0.21\eta^{-1}$. The intercept (0.009 ps^{-1} or 9×10^9 s^{-1}) indicates that in a solvent of infinite viscosity, τ_g^{-1} is reduced significantly. The linear dependence of τ_g^{-1} on η^{-1} supports the general conclusion that the Kramers−Smoluchowski description

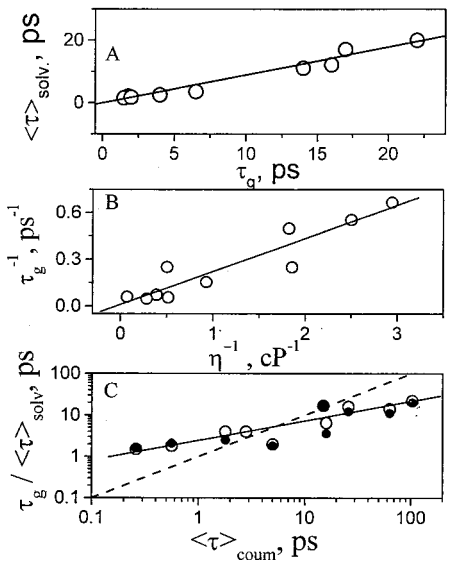

Figure 9. Correlation between τ_g, $\langle\tau\rangle_{solv}$, and $\langle\tau\rangle_{coum}$ in different solvents. (A) Linear correlation between $\langle\tau\rangle_{solv}$ and τ_g. (B) Rate of formation of the TICT state (τ_g^{-1}) is linearly correlated with the inverse of the solvent viscosity, η^{-1}. The straight line is the linear fit function: $\tau_g^{-1} = 0.009 + 0.21\ \eta^{-1}$. (C) Linear correlation between τ_g (○) or $\langle\tau\rangle_{solv}$ (●) and $\langle\tau\rangle_{coum}$. The solid line represents the fit function $\tau_g = 2.45\langle\tau\rangle_{solv}$,$^{0.47}$ and the dashed line represents the unit slope of the plot τ_g or $\langle\tau\rangle_{solv}$ vs $\langle\tau\rangle_{coum}$ or the case τ_g or $\langle\tau\rangle_{solv} = \langle\tau\rangle_{coum}$.

holds in the present case with a frequency-independent friction characterized by the bulk viscosity of the solvent. This simple η^{-1} dependence of the barrier crossing process would correspond to a process with a much flatter and lower energy barrier.[3,50] The exponential evolution of the transient species also supports the presence of the low-energy barrier for the interconversion process. The barrier acts as a bottleneck of the reaction and the barrier crossing process is largely controlled by the viscosity of the medium.

Figure 9C shows that τ_g is also reasonably well correlated with $\langle\tau\rangle_{coum}$, the average (integral) solvation times of the dipolar solvation probe, C-153.[9,51] The solvation times of C-153 have been employed here because they have been considered to represent the best measures of the time scales of polar solvation currently available, since these times are in generally good agreement with predictions of dielectric continuum models of solvation.[45] The solid line in Figure 9C represents the linear fit function: $\log(\tau_g) = 0.39 + 0.47\ \log(\langle\tau\rangle_{coum})$.

It is now important and interesting to compare the intramolecular charge-transfer time, τ_g, and the solvation time, $\langle\tau\rangle_{solv}$, observed here to the previously reported values in similar kinds of systems and also the relation between these parameters. Intramolecular electron-transfer reaction in bianthryl, which has been studied by Barbara and co-workers, provides the most convincing evidence for dynamical solvent-controlled intramolecular electron-transfer process.[8,52] The average electron-transfer time (τ_{et}) in the S_1 state of this molecule and the average solvation time, $\langle\tau\rangle_{solv}$ are close to an equality in each solvent. The modeling performed by these workers indicates that the intramolecular electron-transfer process in bianthryl is more or less barrierless in the polar solvents studied by them. Recently, Maroncelli and co-workers reported their study on the solvent dependence of excited-state intramolecular electron transfer in a donor-substituted acridinium dye, which has been presumed to have a slightly larger activation barrier in the reaction.[45] In this molecule, the lifetimes of the LE → CT conversion process (τ_{ct}) are uniformly greater than the average solvation times, $\langle\tau\rangle_{solv}$. Also, as the solvation time of the solvent increases, the difference between τ_{ct} and $\langle\tau\rangle_{solv}$ decreases, resulting in an apparent power law, $\tau_{ct} \sim 8.4\langle\tau\rangle_{solv}^{0.65}$, similar to the kind we observe in the case of LDS-821, e.g., $\tau_g \sim 2.45\langle\tau\rangle_{solv}^{0.47}$. According to the theory of Nadler and Marcus this kind of power law dependence of the charge-transfer rate on the solvent polarization relaxation time may indicate that the fluctuations in the intramolecular modes of the molecule make the dominant contribution to the reaction process as compared to the solvation of the excited state.[53] In case the solvation is controlling the observed dynamics, the experimental data should fall on the line of unit slope in the plot of τ_g as a function of τ_L or $\langle\tau\rangle_{coum}$, as shown by the dashed line in Figure 9C. As the contributions from the intramolecular modes toward the control of the charge-transfer process increase, i.e., $\lambda_i > \lambda_0$ (λ_i and λ_0 are the reorganization energies due to intramolecular modes and solvation, respectively), the slope is predicted to decrease. In the limit $\lambda_i/\lambda_0 \rightarrow \infty$, solvation does not contribute to the reaction process at all and the reaction rate becomes independent of a change in τ_L. A deviation of the slope of the linear fit function in the plot τ_g as a function of $\langle\tau\rangle_{coum}$ from unity (Figure 9C) indicates that solvation plays a very minor role in the charge-transfer reaction process associated with a small barrier. This conclusion is also supported by the linear dependence of τ_g^{-1} on η^{-1} in all kinds of solvents (Figure 9B). Su and Simon reported similar kinds of results for intramolecular CT reactions of DMABN and DEABN in alcohol solutions at low temperatures.[54]

However, in the present case, the average solvation times determined in the fast relaxing solvents, e.g., ACN, DMSO, and DCM, are longer than both τ_L and $\langle\tau\rangle_{coum}$ (Table 2). In slow relaxing solvents the solvation times are shorter than τ_L or $\langle\tau\rangle_{coum}$ and the difference between the two parameters (i.e., $\langle\tau\rangle_{solv}$ and τ_L or $\langle\tau\rangle_{coum}$) increases as the value of the latter increases (Figure 9C). Till today various kinds of probes have been employed by many groups of workers and in a few cases comparisons have also been made between different probes in the same solvent. For example, Su and Simon[54] compared (dimethylamino)benzonitrile (DMABN) and (diethylamino)-benzonitrile (DEABN) in propanol at several temperatures and found a small but consistent difference in their $\langle\tau\rangle_{solv}$ values. They observed that solvation of the methyl analogue, DMABN, is about 15% faster than that of the DEABN probe. Barbara and co-workers[52] have examined several coumarin dyes in a range of solvents at room temperature. They noted that $\langle\tau\rangle_{solv}$ values obtained with C-153 were consistently 20−40% higher than those observed with C-152 in the same solvent. In these two cases the probes compared are very similar, differing mainly in the overall size due to different alkyl substituents peripheral to an aromatic system. Also, Maroncelli and co-workers examined a wide range of probes in two different solvents, *n*-propanol (253 K) and propylene carbonate (220 K), and found much larger differences in dynamics.[37b] For example, the $\langle\tau\rangle_{solv}$ determined using different kinds of probes in *n*-propanol (253 K) have been seen to vary by about 3 times and, further, there appears to have some correlation between $\langle\tau\rangle_{solv}$ and the magnitude of the time dependent Stokes' shift, $\Delta\nu = \nu(0) - \nu(\infty)$. The former was observed to increase with an increase in the latter. This observation led the authors to suggest that the smaller the perturbation involved, the faster the response, i.e., that the solvation response is inherently nonlinear. Since in the case of the LDS-821 molecule, the change in dipole moment due to photoexcitation (9.8 D) is not very large and association with the solvent molecules is also not very strong, as indicated

by the not very large dynamic Stokes' shift, the perturbation induced to the solvent polarization due to photoexcitation of the molecule is obviously small and hence we observe the solvent polarization relaxation time of the solvent faster than τ_L.

5. Conclusion

The solvent dependent shape of the emission spectra of LDS-821 indicates the presence of more than one conformer in the S_1 state. However, the stimulated emission spectrum recorded at ca. 50 ps after photoexcitation represents the emission from a single conformer, which is a twisted intramolecular charge-transfer (TICT) state. Investigation of the relaxation dynamics of the S_1 state of the dye in subpicosecond time domain in different kinds of solvents shows the presence of at least two kinds of emission. The emission band at 750 nm grows very fast with less than 1 ps growth lifetime but decays slowly with the same rate as the emission band concomitantly occurring at >800 nm grows. Following the theoretical calculations of the potential energy surfaces in the S_1 state of the similar kinds of cyanine dyes by Robb and co-workers,[47] the early time dynamics representing the growth of the 750 nm emission band has been proposed to be due to the relaxation occurring in the valley-like FC region, fully dominated by the barrierless symmetric skeletal deformation mode, leading to the formation of the LE state. The LE state subsequently undergoes a barrier crossing process to form the TICT state via the torsional motion about the only free double bond in the dye molecule. The simple $1/\eta$ dependence of the rate of formation of the TICT state, τ_g^{-1}, indicates that the barrier corresponds to a much flatter and low-energy one. The emission band due to the TICT state revealed the dynamic Stokes' shift in polar media, and from the time dependence of the frequency maximum of the stimulated emission, the average lifetimes of the solvation, $\langle\tau\rangle_{solv}$, for the TICT state in a few of the polar solvents have been measured. τ_g and $\langle\tau\rangle_{solv}$ show linear correlation to each other. However, the latter is longer than the solvation time, $\langle\tau\rangle_{coum}$, which has been determined using a near ideal probe, coumarin-153, in fast relaxing solvents with shorter longitudinal relaxation times. But $\langle\tau\rangle_{solv}$ becomes shorter than $\langle\tau\rangle_{coum}$ in the slow relaxing solvents having longer solvation or longitudinal relaxation times. Since the change in dipole moment due to formation of the TICT state with respect to the ground state is not very large ($\Delta\mu = 9.8$ D), the perturbation to the solvent dipole orientation due to its formation is not very large. Probably, this is the reason for the very fast solvation process of the newly formed TICT state. In addition, in this molecule the intramolecular modes probably control the barrier crossing process rather than the solvent motions.

Acknowledgment. We gratefully acknowledge Prof. N. Periasamy of Tata Institute of Fundamental Research, Mumbai, for his help in measuring the fluoresecence lifetimes of LDS-821 by the single photon counting method and Dr. T. Mukherjee, Head, RC&CD, and Dr. A. V. Sapre, Head, Chemical Dynamics Section, RC&CD, for many stimulating discussions and constant encouragement during this work.

References and Notes

(1) Fleming, G. R. *Chemical Applications of Ultrafast Spectroscopy*; Oxford University Press: Oxford, 1986.

(2) Zewail, A. H. *Femtochemistry and Femtobiology: Ultrafast Reaction Dynamics at Atomic Scale Resolution*; Sundstrom, V., Ed.; Imperial College Press: London, 1997; p 1.

(3) *Ultrafast Reaction Dynamics and Solvent effects*; Gaduel, Y.; Rossky, P. J. Eds.; American Institute of Physics: New York, 1994.

(4) Simon, J. D., Ed. *Ultrafast Dynamics of Chemical Systems*; Kluwer Academic Publisher: Dordercht, The Netherlands, 1994.

(5) *Activated Barrier Crossing*; Fleming, G. R., Hanggi, P., Eds.; World Scientific: Singapore, 1993.

(6) Bhattacharya, K.; Chowdhury, M.; *Chem. Rev.* **1993**, *93*, 507.

(7) Simon, J. D. *Acc. Chem. Res.*, **1988**, *21*, 28.

(8) (a) Barbara, P. F.; Walker, G. C.; Smith, T. P. *Science* **1992**, *256*, 975. (b) Barbara, P. F.; Jarzeba, W. *Adv. Photochem*. **1990**, *15*, 1.

(9) Horng, M. L.; Gardecki, J. A.; Papazyan, A.; Maroncelli, M. *J. Phys. Chem*. **1995**, *99*, 17311.

(10) (a) Sension, R. J.; Szarka, A. Z.; Hochstrasser, R. M. *J. Chem. Phys.* **1992**, *97*, 5239. (b) Sension, R. J.; Repinec, S. T.; Szarka, A. Z.; Hochstrasser, R. M. *J. Chem. Phys.* **1993**, *98*, 6291. (c) Szarka, A. Z.; Pugliano, N.; Palit, D. K.; Hochstrasser, R. M. *Chem. Phys. Lett*. **1995**, *240*, 25. (d) Pederson, S.; Benares, L.; Zewail, A. H. *Chem. Phys. Lett*. **1992**, *97*, 8801. (e) Waldeck, D. H. *Chem. Rev.* **1991**, *91*, 415.

(11) Elsasser, T.; Kaiser, W. *Annu. Rev. Phys. Chem*. **1991**, *42*, 83.

(12) Schlutz, K. E.; Russel, J.; Harris, C. B. *J. Chem. Phys*. **1992**, *97*, 5431.

(13) Nikowa, L.; Schwarzer, D.; Troe, J. *J. Chem. Phys.* **1995**, *233*, 303.

(14) (a) Owrutsky, J. C.; Raftery, D.; Hochstrasser, R. M. *Annu. Rev. Phys. Chem*. **1994**, *45*, 519. (b) Pugliano, N.; Szarka, A. Z.; Palit, D. K.; Hochstrasser, R. M. *J. Chem. Phys.* **1993**, *99*, 7273.

(15) (a) Ashworth, S. H.; Hasche, T.; Woerner, M.; Elsasser, T. *J. Chem. Phys.* **1996**, *104*, 5761. (b) Ashworth, S. H.; Reiddle, E.; Woerner, M.; Elsasser, T. *Chem. Phys. Lett.* **1995**, *244*, 164.

(16) (a) Martini, I.; Hartland, G. V. *J. Phys. Chem*. **1996**, *100*, 19764. (b) Martini, I.; Hartland, G. V. *Chem. Phys. Lett*. **1996**, *258*, 180.

(17) Sension, R. J.; Szarka, A. Z.; Hochstrasser, R. M. *J. Chem. Phys.* **1992**, *97*, 5239.

(18) (a) Naber, A.; Fischer, U. C.; Kirchner, S.; Dziomba, T.; Kollar, G.; Chi, L. F.; Fuchs, H. *J. Phys. Chem. B* **1999**, *103*, 2709. (b) Gretchikhine, A.; Schweiter, G.; Van der Auweraer, M.; De Keyzer, R.; Van den Brouchke, D.; De Schryver, F. C. *J. Appl. Phys*. **1999**, *85*, 1283. (c) Hammilton, J. F. In *The Theory of the Photographic Processes*, 4th ed.; James, T. H., Ed.; Macmillan: New York, 1977; p 235.

(19) (a) Fabian, J.; Nakazumi, H.; Matsuoka, M. *Chem. Rev.* **1992**, *92*, 1197. (b) Kaliteevskaya, E. N.; Razumova, T. K.; Tarnovskii, A. N. *Opt. Spectrosc*. **1999**, *1*, 126.

(20) (a) Mujumder, S. R.; Mujumder, R. B.; Grant, C. M.; Waggoner, A. S. *Bioconjugate Chem.* **1996**, *7*, 356. (b) Seifert, J. L.; Connor, R. E.; Kushon, S. A.; Wang, M.; Armitage, B. A. *J. Am. Chem. Soc*. **1999**, *121*, 2987. (c) Nunnaly, B. K.; He, H.; Li, L. C.; Tucker, S. A.; McGown, L. B. *Anal. Chem*. **1997**, *69*, 2392.

(21) Fromhertz, P.; Dambcher, K. H.; Ephardt, H.; Lambcher, A.; Muller, C. O.; Neigle, R.; Schaden, H,; Schenk, O.; Vetter, T. *Ber. Bunsen-Ges. Phys. Chem.* **1991**, *95*, 1333.

(22) (a) Berndt, K.; Durr, H.; Feller, K.-H. *Z. Phys. Chem. Leipzig* **1987**, *268*, 250. (b) Levitus, M.; Martin Negri, R.; Aramendia, P. F. *J. Phys. Chem.* **1995**, *99*, 14231. (c) Chibsov, A. K.; Zakharova, G. H. *J. Chem. Soc., Faraday Trans.* **1996**, *92*, 4917. (d) Murphy, S.; Sauerwein, B.; Drickmer, H. G.; Schuster, G. B. *J. Phys. Chem.* **1994**, *98*, 13476.

(23) (a) Aramendia, P. F.; Martin Negri, R.; San Roman, E. *J. Phys. Chem.* **1994**, *98*, 3165. (b) Rulliere, C. *Chem. Phys. Lett.* **1976**, *43*, 303.

(24) Castner, E. W., Jr.; Maroncelli, M.; Fleming, G. R. *J. Chem. Phys.* **1987**, *86*, 1090.

(25) (a) Cho, M.; Rosenthal, S. J.; Scherer, N. F.; Ziegler, L. D.; Fleming, G. R. *J. Chem. Phys.* **1992**, *96*, 5033. (b) Rosenthal, S. J.; Xie, X.; Du, M.; Fleming, G. R. *J. Chem. Phys.* **1991**, *95*, 4715.

(26) Van der Meer, M. J.; Zhang, H.; Rettig, W.; Glasbeek, M. *Chem. Phys. Lett.* **2000**, *320*, 673.

(27) Borden, C. J.; Rosenthal, S. J.; Shank, C. V. *J. Phys. Chem. A* **1999**, *103*, 10506.

(28) Kovalenko, S. A.; Ernsting, N. P.; Ruthmann, J. *J. Chem. Phys.* **1997**, *106*, 3504.

(29) Smith, N. A.; Meech, S. R.; Rubtsov, I. V.; Yoshihara, K. *Chem. Phys. Lett.* **1999**, *303*, 209.

(30) Zhong, Q.; Wang, Z,; Sun, Y.; Zhu, Q,; Kong, F. *Chem. Phys. Lett*. **1996**, *248*, 277.

(31) Bingemann, D.; Ernsting, N. P. *J. Chem. Phys*. **1995**, *102*, 2691.

(32) Sperber, P.; Spangler, W.; Meier, B.; Penzkofper, A. *Opt. Quantum Electron*. **1988**, *20*, 395.

(33) Palit, D. K.; Pal, H.; Mukherjee, T.; Mittal, J. P. *J. Chem. Soc., Faraday Trans.* **1990**, *86*, 3861.

(34) Periasamy, N.; Doraiswamy, S.; Maiya, G. B.; Venkataraman, B. *J. Chem. Phys.* **1988**, *88*, 681.

(35) Bhasikuttan, A. C.; Singh, A. K.; Palit, D. K.; Sapre, A. V.; Mittal, J. P. *J. Phys. Chem. A* **1998**, *102*, 3470.

(36) Brackmann, U. *Lambdachrome Laser Grade Dyes*; Lambda Physok Gmbh: Gottingen, 1986; p III−181.

(37) (a) Reynolds, L.; Gardecki, J. A.; Frankland, J. V.; Horng, M. L.; Maroncelli, *J. Phys. Chem.* **1996**, *100*, 10337. (b) Maroncelli, M. *J. Mol. Liq.* **1993**, *57*, 1.

(38) (a) Reichardt, C. *Solvents and Solvent Effects in Organic Chemistry*; VCH: Weinheim, FRG, 1988. (b) Dimroth, K.; Reichardt, C. *Z. Anal. Chem.* **1966**, *215*, 344. (c) Parker, A. J. *Adv. Phys. Org. Chem.* **1967**, *5*, 173; *Chem. Rev.* **1969**, *69*, 1.

(39) (a) Lippert, E. *Z. Naturforsch.* **1955**, *A10*, 541. (b) Mcrae, E. G. *J. Phys. Chem.* **1957**, *61*, 562. (c) Mataga, N.; Kaifu, Y.; Koizumi, M. *Bull. Chem. Soc. Jpn.*, **1955**, *28*, 690.

(40) Van der Zwan, G.; Hynes, J. T. *J. Phys. Chem.* **1985**, *89*, 4181.

(41) Mazurenko, Y. T.; Bakshiev, N. G. *Opt. Spectrosc.* **1970**, *28*, 490.

(42) Bagchi, B.; Oxotoby, D. W.; Fleming, G. R. *Chem. Phys.* **1984**, *86*, 257.

(43) Van der Meulen, P.; Zhang, H.; Jonkman, A. M.; Glasbeek, M. *J. Phys. Chem.* **1996**, *100*, 5367.

(44) Kang, T. J.; Jarzeba, W.; Barbara, P. F.; Fonseca, T. *J. Chem. Phys.* **1990**, *149*, 81.

(45) Horng, M. L.; Dahl, K.; Jones, G., II.; Maroncelli, M. *Chem. Phys. Lett.* **1999**, *315*, 363.

(46) (a) Gretchikhine, A.; Schweiter, G.; Van der Auweraer, M.; De Keyzer, R.; Vandeubrouchke, D.; De Schryver, F. C. *J. Appl. Phys.* **1999**, *85*, 1283. (b) Khimaenko, V.; Chibisov, A. K.; Gorner, H. *J. Phys. Chem. A* **1997**, *101*, 7304. (c) Tatikolov, A. S.; Dzhulibekov, K. S.; Shevedoua, L. A.; Kuzmin, V. A. *J. Phys. Chem.* **1995**, *99*, 6525. (d) Shalyun, M. R.; Serpone, N. V. *J. Phys. Chem.* **199**7, *101*, 9877. (e) Khirutdinov, R. F.; Serpone, N. V. *J. Phys. Chem. B* **1997**, *101*, 2602. (f) Yartsev, A.; Alvarez, J. L.; Aberg, U.; Sundstorm, V. *Chem. Phys. Lett.* **1995**, *243*, 281.

(47) Sanchez-Galvez, A.; Hunt, P.; Robb. M. A.; Olivucci, M.; Vreven, T.; Schlegel, H. B. *J. Am. Chem. Soc.* **2000**, *122*, 2911.

(48) (a) Garavelli, M.; Vreven, T.; Celani, P.; Bernardi, F. Robb. M. A.; Olivucci, M. *J. Am. Chem. Soc.* **1998**, *120*, 1285. (b) Garavelli, M.; Negri, F.; Olivucci, M. *J. Am. Chem. Soc.* **1999**, *121*, 1023. (c) Garavelli, M.; Celani, P.; Bernardi, F.; Robb. M. A.; Olivucci, M. *J. Am. Chem. Soc.* **1997**, *119*, 6891.

(49) Laermer, F.; Elsasser, T.; Kaiser, W. *Chem. Phys. Lett.* **1989**, *156*, 535.

(50) (a) Nikowa, L.; Schwarzer, D.; Troe, J.; Schroeder, J. *J. Chem. Phys.* **1992**, *97*, 4827. (b) Gehrke, Ch.; Schroeder, J.; Schwarzer, D.; Troe, J.; Voss, F. *J. Chem. Phys.* **1990**, *92*, 4805. (c) Schroeder, J.; Schwarzer, D.; Troe, J.; Voss, F. *J. Chem. Phys.* **1990**, *93*, 2393.

(51) (a) Zhou, H.-X. *Chem. Phys. Lett.* **1989**, *164*, 285. (b) Poornimadevi, C. S.; Bagchi, B. *Chem. Phys. Lett.* **1990**, *168*, 276.

(52) (a) Nagarajan, V.; Brearley, A. M.; Kang, T. J.; Barbara, P. F. *J. Chem. Phys.* **1987**, *86*, 3183. (b) Kong, T. J.; Kahlow, M. A.; Giser, D.; Swallen, S.; Nagarajan, V.; Jarzeba, W.; Barbara, P. F. *J. Phys. Chem.* **1988**, *92*, 6800. (c) Tominaga, K.; Walker, G. C.; Kang, T. J.; Barbara, P. F.; Fonseca, T. *J. Phys. Chem.* **1991**, *95*, 10485.

(53) Nadler, W.; Marcus, R. A. *J. Chem. Phys.* **1987**, *86*, 3906.

(54) Su, S.-G.; Simon, J. D. *J. Chem. Phys.* **1988**, *89*, 908.